NUCLEAR INSTRUMENTS AND METHODS 144 (1977) 215-224 ; © NORTH-HOLLAND PUBLISHING CO.

ON THE DETERMINATION OF FAST NEUTRON SPECTRA WITH ACTIVATION TECHNIQUES; ITS APPLICATION IN A FUSION REACTOR BLANKET MODEL

L. KUIJPERS, R. HERZING, P. CLOTH, D. FILGES and R. HECKER

Institut für Reaktorentwicklung, Kernforschungsanlage Jülich, Association Euratom–KFA, 5170 Jülich, W. Germany

Received 21 February 1977

A suitable method for the determination of neutron spectra in a CTR-blanket model is the activation technique with threshold detectors. Unfolding of the results from the measurements yields information on the neutron spectrum in the energy range of 2.0–14.1 MeV. The SAND II unfolding program is applied; some investigations have been performed to show the influence of different data files, and of errors in cross sections and activity values.

Comparisons of experimental results with values calculated by a Monte Carlo program are presented and discussed.

1. Introduction

The choice of measuring techniques for the determination of fast neutron spectra produced from the interaction of 14 MeV source neutrons with "blanket" materials is limited.

For measurements two groups of methods could be used:

A) Measurements of fast neutron flux densities with activation detectors, and in particular threshold detectors, show good prospects for the discrimination between neutrons of different energies. Activation detectors are extremely small in size, so that they do not disturb the neutron flux. From the measurements with these detectors the neutron spectra may be derived by applying a suitable unfolding method[1,2]).

B) Proton recoil techniques using gas filled counters and organic scintillators are also often used for fast neutron spectroscopy. In this case spectra can also be obtained with the help of an unfolding method. Both kinds of detectors, however, have a poor resolution at the 14 MeV neutron energy and are sensitive against γ-radiation; in addition they are normally not able to deliver the spectrum with one single measurement over the whole energy range. Furthermore they need a rather large space, thus causing a disturbance in the spectrum. Semiconductor detectors – especially semiconductor sandwich devices using a ^{6}LiF layer as converter – and ^{6}LiI(Eu) crystals deliver direct information and discriminate against competing reactions by high energy neutrons, due to the Q-value of +4.78 MeV of the ^{6}Li(n, α)t reaction. However, for the determination of the neutron spectrum in the lower energy range (below 10 MeV), this detector cannot be used, due to competing reactions in the silicon diodes themselves[3]). In the ^{6}LiI(Eu) crystal competing effects are due to the ^{6}Li(n, αn')d reaction. Furthermore the crystal has to be cooled down to 77 K to achieve a good resolution, resulting in a considerable amount of material, which will disturb the neutron flux. On account of their disadvantages these detectors were not used in the work described in this paper.

It was decided to use for this investigation the well known foil activation technique. Foil materials were selected according to the following criteria:

1) The cross section for the activation reaction should be well known in the energy range of interest.
2) The produced radionuclides should be gamma-emitters since gamma measurements may be carried out with good precision and by selection of a representative "line" one can discriminate against background caused by γ-radiation from other nuclides produced.
3) Accurate data on gamma-ray abundances of the produced radionuclides should be available.
4) The half-life of the radionuclide should be known with less than 2% uncertainty; its half-life should lie in the range of about 10 min up to some weeks, taking into consideration the neutron source strength.

TABLE 1

Properties of the activation detectors, used in the model blanket experiment. The γ-energies, given in this table, are those which are used in the measurements. + = annihilation radiation, ○ = γ abundance if all positions are converted into γ-radiation, × = β radiation with a maximum of keV. The nuclear properties are taken from Lederer[15]).

Material	Thickness (mm)	Reactions of interest	Isotopic abundance (at. %)	Half-life	γ-energy (MeV)	γ-abundance (%)	Threshold (MeV)
F (teflon)	1.0	$^{19}F(n,2n)^{18}F$	100.0	109.7 min	+0.511	○194	11.6
Na(Na_2CO_3)	1.0	$^{23}Na(n,\gamma)^{24}Na$	100.0	15.0 h	1.368	100	–
Mg	0.127	$^{24}Mn(n,p)^{24}Na$	78.7	15.0 h	1.368	100	6.0
Al	0.762	$^{27}Al(n,\alpha)^{24}Na$	100.0	15.0 h	1.368	100	4.9
Al	0.762	$^{27}Al(n,p)^{27}Mg$	100.0	9.46 min	0.84–1.01	100	3.8
Mn	0.1	$^{55}Mn(n,\gamma)^{56}Mn$	100.0	2.56 h	0.84	99	–
Fe	0.127	$^{56}Fe(n,p)^{56}Mn$	91.7	2.56 h	0.84	99	4.9
Co	0.1	$^{59}Co(n,\alpha)^{56}Mn$	100.0	2.56 h	0.84	99	5.2
Ni	0.5	$^{58}Ni(n,2n)^{57}Ni$	67.9	36.0 h	1.37	86	13.0
Ni	0.5	$^{58}Ni(n,p)^{58}Co$	67.9	71.6 h	0.81	99	1.9
Cu	0.254	$^{63}Cu(n,2n)^{62}Cu$	30.9	9.8 min	+0.511	○195	11.9
Cu	0.254	$^{63}Cu(n,\gamma)^{64}Cu$	30.9	12.7 h	+0.511	○37.8	–
Cu	0.254	$^{65}Cu(n,2n)^{64}Cu$	69.1				
Zn	0.254	$^{64}Zn(n,p)^{64}Cu$	48.8	12.7 h	+0.511	○37.8	2.0
In	0.254	$^{115}In(n,n')^{115m}In$	95.7	4.50 h	0.335	48	0.5
In	0.254	$^{115}In(n,\gamma)^{116}In$	95.7	54.0 min	1.09–1.29	80	–
I	1.0	$^{127}I(n,2n)^{126}I$	100.0	13.0 d	0.667	33	9.3
Au	0.1	$^{197}Au(n,2n)^{196}Au$	100.0	6.18 d	0.33–0.35	25–94	8.6
Au	0.1	$^{197}Au(n,\gamma)^{198}Au$	100.0	2.70 d	0.412	95	–
Li(Li_2CO_3)	3.0	$^{6}Li(n,\alpha)t$	7.42	12.3 a	×0–0.019	100	–
Li(Li_2CO_3)	3.0	$^{7}Li(n,\alpha n')t$	92.58	12.3 a	×0–0.019	100	3.8

5) The various reaction cross sections should cover the entire energy range of interest.
6) The foil material should be available in high purity to reduce disturbing reactions.. Sometimes, when other isotopes cause many competing reactions it may be required to use enriched materials.
7) It should be possible to process the material into a thin foil with sufficient mechanical stability.
8) It will be advantageous if the reaction cross sections are included in cross section-data files, e.g. ENDF/B-III or IV.

The properties of the activation detectors which are available for such measurements are summarized in table I.

2. The determination of neutron spectra with activation techniques

2.1. THE APPLICATION ON A LITHIUM BLANKET MODEL FOR THE FUSION REACTOR

In future a fusion reactor will be based on the deuterium–tritium fusion reaction: $D+T \rightarrow {}^4He+n$. Of the reaction energy 80% (14 MeV) appears as kinetic energy of the emitted neutron. Whereas the deuterium necessary for this reaction can be won from the ocean in high quantities, the tritium, needed for this fuel cycle, cannot be found in sufficient quantities in nature. It has, therefore, to be bred via reactions, induced by the neutrons produced by the D–T reactions. Lithium is most suited for this tritium production due to its relatively high cross section for (n, t) reactions and its low cross section for parasitic absorption. It is possible to breed more than one tritium atom per neutron and to enlarge the total energy production in this way. For this tritium breeding the plasma volume has to be surrounded by a blanket consisting of lithium in some form. A good approximation for the toroidal geometry of a fusion reactor blanket is a cylinder. Based on this geometry a blanket model, consisting of pure lithium, has been constructed[4]). Resulting from optimization studies this cylindrical blanket has the dimensions of 1.2 m in diameter and 1.2 m in axial length; the model contains 692 kg of pure lithium metal.

An axial central channel of 0.2 m in diameter has been provided to give room for the introduction of the tube of an accelerator which produces 14 MeV neutrons by bombarding a tritium target with 300 keV deuterons (maximum neutron production rate of 2×10^{11} s^{-1}). In this way a point source of fusion neutrons can be simulated. Twelve radial channels – 40 mm in width – to insert detectors or lithium pellets, are distributed over the surface of the cylinder (see fig. 1).

From considerations on the energy of the produced neutrons and the distribution around the target it follows that accurate comparisons can be made in the 90° direction with respect to the deuteron beam[5]). In this article, therefore, comparisons of experimental results and calculated values of neutron spectra are only given for the central radial channels of the blanket model.

2.2. Experimental procedure

Unfolding methods require as main input data measured activities of different reactions converted into saturation activities. This saturation activity is defined as the number of decays per second and per nucleus of interest in the detector, related to a constant neutron source production rate of 1 s^{-1}. At the reference position $R = 0.10$ m in the blanket model the saturation activities for the used reactions are determined from simultaneous measurements. At the other positions the saturation activities are calculated from the simultaneous measurements (at the position $R = 0.10$ m) and from relative space dependent measurements.

For such relative measurements a number of activation detectors, consisting of the same material, is distributed in the blanket (at a maximum of nine detectors); during irradiation the position of the source is monitored by teflon foils in the axial channel of the blanket to relate all measurements to exactly the same source position. This is shown in fig. 2.

The activities of the radionuclides produced during blanket irradiations, were determined with a 3″×3″ NaI(Tl) detector, shielded by 0.15 m lead on all sides. This detector was connected with a 512-channel pulse height analyzer. The efficiency

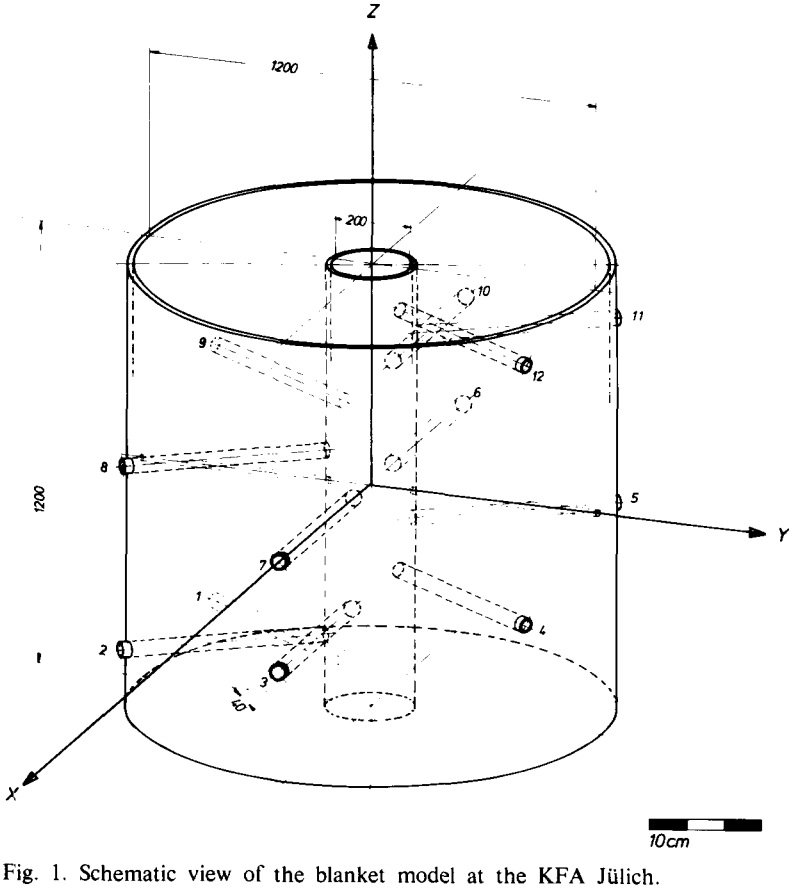

Fig. 1. Schematic view of the blanket model at the KFA Jülich.

calibration of the counting equipment was carried out with various calibration standards; the measured efficiencies were in good agreement with values given by Chinaglia[6]). The energy dependence of the efficiency – with about 1% relative uncertainty – obtained by Chinaglia was used to interpolate between the calibration points.

The NaI(Tl) detector, although having a poor resolution as compared with a Ge(Li) detector, is preferred because of its higher efficiency; the necessary irradiation time can be shorter in this way.

The neutron source output is measured by determining the amount of ^{57}Ni produced via the high threshold ^{58}Ni(n, 2n)^{57}Ni reaction (13.2 MeV). ^{57}Ni is measured in the same way as the other nuclides produced so that the systematic error in the detector efficiency will be eliminated for a large part; only the relative uncertainty from Chinaglia's measurements, as given above, remains. The total uncertainty in the saturation activities will be about 2.5–5%. However, the determination of the 14 MeV neutron source output is directly influenced by the uncertainty of the ^{58}Ni(n, 2n)^{57}Ni cross section, which is about 15%. It can be concluded that all saturation activities will have the same systematic uncertainty, caused by the source output determination, of about 15%.

3. Unfolding methods

3.1. General remarks

Several computer programs have been developed to determine neutron spectra using results of activation measurements. These programs are based on a set of equations of the following type:

$$\alpha_i = \int_0^\infty \sigma_i(E)\, \phi_E(E)\, \mathrm{d}E, \qquad i = 1, \ldots, n,$$

in which α_i is the measured saturation activity per nucleus, $\sigma_i(E)$ the energy dependent activation cross section, $\Phi_E(E)$ the spectral flux density per unit energy interval, related to a source production of 1 s^{-1}, and n the number of reactions used in this evaluation.

In the computer programs the number of flux density groups is considerably larger than the number of activation reactions. The programs therefore require an a priori knowledge in the form of an input spectrum. This input should represent all available information about the spectrum from experiments and calculations. Generally, the quality of the output spectrum is influenced by:

- the choice of the input spectrum;
- the choice of the set of activation reactions;

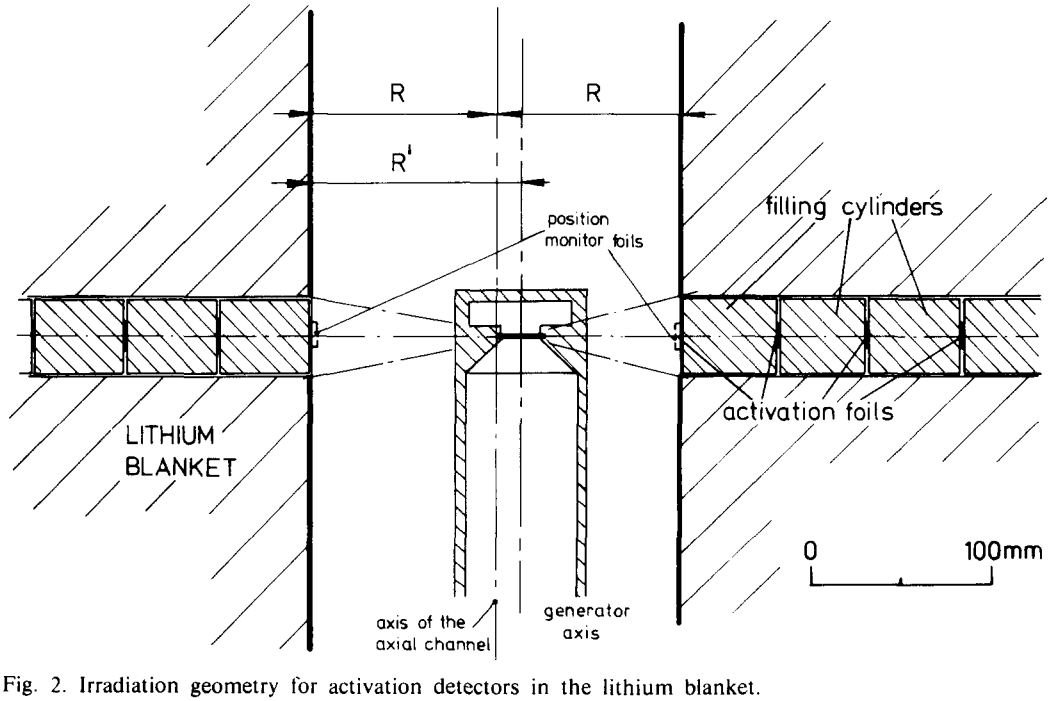

Fig. 2. Irradiation geometry for activation detectors in the lithium blanket.

- the errors in the measured activities used as input data;
- the uncertainties in the cross sections of the activation reactions.

3.2. The SAND II unfolding method

Several unfolding methods were compared and tested on proper functioning within the scope of our blanket experiment; the results are given elsewhere[5]). From these comparisons the SAND II method was selected, as an acceptable output spectrum was obtained even when there was no extra information in the input spectrum. Special tests were also performed with the SAND II program[5]).

This program was developed by McElroy and coworkers[7]) and applies a non-linear adjustment to the input spectrum or calculated spectrum at each iteration step. The energy range of the solution-spectrum covers the range from 10^{-10} MeV up to 18 MeV, in 620 energy groups. The program calculates for each activation reaction a ratio of measured to calculated activity and a deviation parameter D being the standard deviation of all ratios.

Iteration steps are performed until this deviation parameter has reached a certain input value or if a prefixed number of iterations has been performed. In this experiment the input value is taken to be 5% considering the errors in the measured activities; 20 iteration steps is the other limiting value. The iteration steps are also stopped, if 'stability' is reached: this means if $(D^k - D^{k+1})/D^k < \varepsilon$; for ε the value of 0.01 is chosen.

3.3. Some remarks on the input data

In this experiment a reference blanket spectrum is defined. This flux density spectrum is the average of a number of calculated blanket spectra at different positions (calculated with the Monte Carlo program, MORSE mentioned in section 4, and equally spaced between 0.10 and 0.60 m in radial distance). Some smoothing has been applied on this spectrum to reduce improbable flux density variations over the energy range. It can thus be characterized as a spectrum which shows all typical flux density patterns, known from calculations. Numerical values for this spectrum are given elsewhere[5]). To check the dependence of the output on the input spectrum also an input spectrum is taken which contains no a priori information at all: a so called constant flux density per unit energy spectrum. Spectrum unfolding can be carried out with the original SAND II cross section library; in this case the Petten version, the so called CCC 112B library, is taken[8]).

Recently however, a newer file, based on the ENDF/B-IV data file, was published[9]). A certain number of cross sections [i.e. ^{63}Cu(n, 2n), ^{62}Cu, ^{24}Mg(n,p)^{24}Na, ^{64}Zn(n,p)^{64}Cu and ^{55}Mn(n,γ)^{56}Mn] is not available on this file. In the spectrum unfolding in this experiment, therefore, also a "ENDF/B-IV+CCC 112B" library is used of which four reactions come from the CCC 112B library. Both libraries do not contain the cross section for the ^{19}F(n, 2n)^{18}F reaction; in this experiment the cross section is taken from a publication by Shiokawa[10]).

4. Theoretical procedure

The theoretical treatment of the blanket problems has to deal with high energetic neutrons and

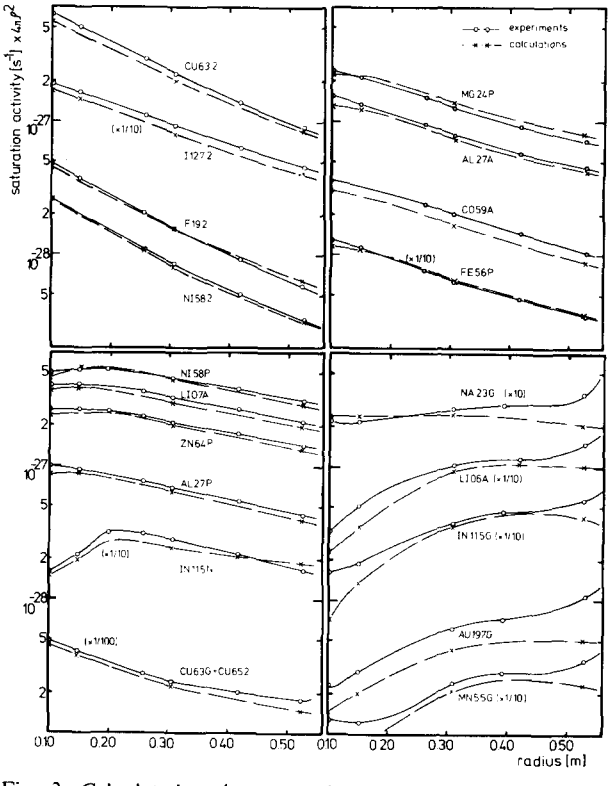

Fig. 3. Calculated and measured space dependent saturation activities (per relevant nucleus per second) at a neutron source production of one 14.1 MeV neutron per second for various activation reactions in the lithium blanket; ρ is the normalized radius. Each reaction is given by a short notation, e.g. ^{24}Mg(n,p)^{24}Na is written as MG24P.

their interactions with blanket material. Experience drawn from other investigations shows that Monte Carlo methods describe the neutron flux in a convenient way. Therefore the neutron flux density distribution and space dependent saturation activities have been calculated using the three dimensional Monte Carlo code MORSE [11]). The problems have been run with a 99-group GAM II P_3 cross section library. The cross section for the neutron induced reactions, the energy and angular distributions as well as the resonance parameters for the materials ^{6}Li, ^{7}Li, and stainless steel have been taken from the ENDF/B-III data file. The group cross sections have been generated with the code SUPERTOG [12]). In the MORSE runs the histories of 160 000 source particles have been observed. The neutron flux in the relevant regions has been calculated by the neutron track length estimator technique[13]). From these neutron spectra the space dependent tritium production has been calculated using the ENDF/B-III cross sections for the lithium isotopes; the saturation activities have been calculated using the "ENDF/B-IV+CCC 112B" library, as mentioned above.

5. Results

In fig. 3 the space dependent saturation activities, measured following the methods given in section 3 and calculated with the Monte Carlo program, are given. The experimental results for three positions in the lithium blanket are also listed in table 2. The neutron source output is determined with the ^{58}Ni(n, 2n)^{57}Ni activation method. To have indications about the deviation of the measured from the calculated activity the average ratio of the measured to calculated activity for various reactions is given in table 3; also an estimation of the uncertainty, determined from the statistical uncertainties of calculations and measurements, is given. To avoid a falling of the curves over several decades in fig. 3 the results are multiplied there with $4\pi\rho^2$, in which ρ is a normalized radius, equal to (r/R); r is the distance from the neutron source and R the reference radius equal to 0.1 m.

The saturation activities of the lithium reactions, which can be derived from the tritium production in the blanket model, were measured with radiochemical methods[14,15]). In fig. 4 the tritium production in natural lithium, separated to ^{7}Li and ^{6}Li, is given as measured with pellets containing the isotopes in high abundance (95.62 at % ^{6}Li; 99.99 at. % ^{7}Li).

The results can be compared to the Monte Carlo calculated values, also given in fig. 4. The

TABLE 2

Measured saturation activities at three positions in the lithium blanket (s^{-1}).

Reactions	Position $R = 0.100$ m	$R = 0.308$ m	$R = 0.528$ m
^{58}Ni(n,2n)^{57}Ni	2.089 E-29 ± 2.9%	7.111 E-31 ± 3.9%	9.139 E-32 ± 4.6%
^{6}Li(n,α)t	2.659 E-28 ± 4.2%	8.718 E-29 ± 4.4%	4.273 E-29 ± 5.2%
^{7}Li(n,αn')t	3.138 E-28 ± 4.8%	2.695 E-29 ± 6.1%	6.134 E-30 ± 7.0%
^{19}F(n,2n)^{18}F	3.899 E-29 ± 4.5%	1.327 E-30 ± 4.9%	1.706 E-31 ± 4.9%
^{23}Na(n,γ)^{24}Na	1.779 E-29 ± 5.9%	2.307 E-30 ± 6.4%	1.021 E-30 ± 6.6%
^{24}Mg(n,p)^{24}Na	1.895 E-28 ± 4.7%	1.083 E-29 ± 4.6%	2.026 E-30 ± 4.7%
^{27}Al(n,α)^{24}Na	1.227 E-28 ± 2.5%	6.661 E-30 ± 2.8%	1.321 E-30 ± 3.0%
^{27}Al(n,p)^{27}Mg	7.936 E-29 ± 2.5%	5.730 E-30 ± 2.7%	1.282 E-30 ± 3.0%
^{55}Mn(n,γ)^{56}Mn	1.037 E-29 ± 4.0%	2.097 E-30 ± 4.2%	1.041 E-30 ± 4.3%
^{56}Fe(n,p)^{56}Mn	9.995 E-29 ± 4.4%	5.309 E-30 ± 5.1%	1.022 E-30 ± 5.7%
^{58}Ni(n,2n)^{57}Ni	2.089 E-29 ± 2.9%	7.111 E-31 ± 3.9%	9.139 E-32 ± 4.6%
^{58}Ni(n,p)^{58}Co	3.853 E-28 ± 4.0%	3.785 E-29 ± 3.0%	8.931 E-30 ± 3.4%
^{59}Co(n,α)^{56}Mn	2.800 E-29 ± 3.2%	1.697 E-30 ± 6.8%	2.912 E-31 ± 7.0%
^{63}Cu(n,2n)^{62}Cu	4.978 E-28 ± 3.8%	1.863 E-29 ± 4.5%	2.590 E-30 ± 4.5%
^{63}Cu(n,γ)^{64}Cu	3.889 E-28 ± 2.9%	2.091 E-29 ± 3.0%	4.910 E-30 ± 3.5%
^{64}Zn(n,p)^{64}Cu	2.030 E-28 ± 4.0%	1.755 E-29 ± 4.3%	4.076 E-30 ± 4.8%
^{115}In(n,n')^{115}In	1.249 E-28 ± 3.7%	2.395 E-29 ± 4.8%	4.792 E-30 ± 5.2%
^{115}In(n,γ)^{116}In	1.315 E-28 ± 2.4%	3.341 E-29 ± 2.4%	1.665 E-29 ± 2.5%
^{127}I(n,2n)^{126}I	1.549 E-27 ± 3.5%	7.665 E-29 ± 4.8%	1.332 E-29 ± 5.3%
^{197}Au(n,2n)^{196}Au	2.489 E-27 ± 5.3%	1.252 E-28 ± 6.2%	2.072 E-29 ± 7.0%
^{197}Au(n,γ)^{198}Au	1.866 E-28 ± 5.3%	5.429 E-29 ± 6.0%	3.156 E-29 ± 6.7%

TABLE 3

Ratio of the measured saturation activity to the activity, calculated via the Monte Carlo program, averaged over a number of positions in the lithium blanket.

Reaction	Ratio (%)	Reaction	Ratio (%)
$^{7}Li(n,\alpha n')t$	1.075±4.0	$^{58}Ni(n,p)^{58}Co$	1.044±3.0
$^{19}F(n,2n)^{18}F$	0.989±3.5	$^{59}Co(n,\alpha)^{56}Mn$	1.172±4.0
$^{24}Mg(n,p)^{24}Na$	0.948±3.5	$^{63}Cu(n,2n)^{62}Cu$	1.089±3.3
$^{27}Al(n,\alpha)^{24}Na$	1.086±2.9	$^{63}Cu(n,\gamma)^{64}Cu$	1.108±3.0
$^{27}Al(n,p)^{27}Mg$	1.095±2.9	$^{64}Zn(n,p)^{64}Cu$	1.084±3.4
$^{56}Fe(n,p)^{56}Mn$	0.995±2.4	$^{115}In(n,n')^{115m}In$	1.045±3.3
$^{58}Ni(n,2n)^{57}Ni$	1.025±3.1	$^{127}I(n,2n)^{126}I$	1.159±3.3

$^{7}Li(n, \alpha n')t$ reaction has its threshold at about 2.5 MeV whilst the $^{6}Li(n, \alpha)t$ reaction is caused mainly by thermal and epithermal neutrons.

From table 3 and figs. 3 and 4 the following can be concluded:

1) There is a good agreement, within the limits for systematical errors, between the calculated and measured activities for the threshold reactions; only slight differences between the shape of the curves can be observed for the $^{115}In(n, n')^{115m}In$ reaction.
2) A comparison between calculated and measured activities for the $^{59}Co(n, \alpha)^{56}Mn$ and the $^{127}I(n, 2n)^{126}I$ reaction may indicate a systematic error in their cross sections.
3) For the activities from reactions which have their response mainly in the lower energy range some remarkable differences can be observed at the inner and outer region of the blanket (at distances of 0–0.1 m from the steel wall). At the inner side the increase of the tritium production is caused by scattered neutrons from the water in the target jacket and the cooling supplies. At the outer side this is caused by backscattered epithermal neutrons from the experimental room (to capture thermal neutrons the blanket had been covered with a cadmium shield of 1 mm thickness).

With the Monte Carlo program neutron spectra were calculated at the radial positions $R = 0.10$, 0.308 and 0.528 m in the GAM II group structure. These calculated spectra are compared to spectra unfolded with the SAND II program, using only threshold reactions, in the 2.0–14.1 MeV energy range.

1) *Position $R = 0.528$ m*

With 13 saturation activities (from threshold reactions) three SAND II runs were performed, of which the unfolded spectra are shown in fig. 6, following a fixed scheme (see table 4).

From fig. 5 it can be concluded that the neutron flux density in the 2–4 MeV energy range is small-

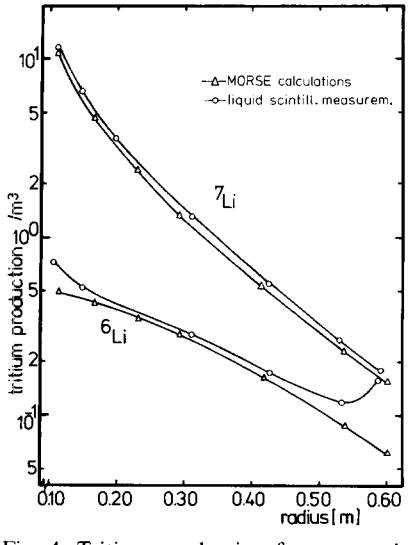

Fig. 4. Tritium production from natural lithium, separated to the ^{6}Li and ^{7}Li isotope, measured with pellets containing the isotopes in high abundance and calculated with the Monte Carlo program.

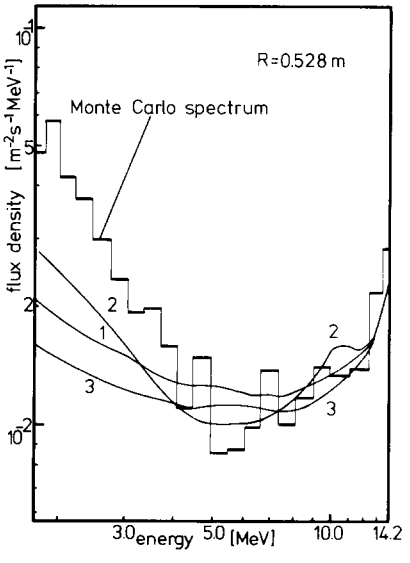

Fig. 5. Results of three SAND II runs and the calculated Monte Carlo spectrum for the position $R = 0.528$ m in the lithium blanket. 1/2 denotes a change of the input spectrum, 1/3 a change of the library.

TABLE 4
Fixed scheme for SAND II runs in the blanket experiment.

Curve	Library	Input spectrum	Iterations	Dev. par.
1	ENDF/B-IV+CCC 112B	constant flux density	9	7.23%
2	ENDF/B-IV+CCC 112B	reference blanket spectrum	7	7.05%
3	CCC 112B	constant flux density	7	8.05%

er in the unfolded spectra compared to the Monte Carlo calculations. The best results are obtained with the reference blanket spectrum as input spectrum; the application of the CCC 112B library gives results which are systematically lower compared to those obtained with the application of the ENDF/B-IV+CCC 112B library.

2) *Position $R = 0.308$ m.*

With 13 saturation activies (from threshold reactions) three SAND II runs were performed following the fixed scheme. The results are shown in fig. 6 (curve 1, 16 iterations, $D = 7.27\%$ curve 2, 14 iterations, $D = 7.09\%$; curve 3, 17 iterations, $D = 7.78\%$). For this position the use of the reference blanket spectrum as input spectrum also yields the best results. The neutron flux density in the unfolded spectrum (curve 2) is slightly smaller compared to the Monte Carlo spectrum, but in general deviations of less than 20% can be observed between these two spectra. The application of the CCC 112B again shows a tendency for lower values in the unfolded spectrum.

3) *Position $R = 0.10$ m.*

With 13 saturation activities (from threshold reactions) three SAND II runs were again performed following the fixed scheme. At this position the neutron flux density in the energy group of source neutrons is extremely large compared to lower energy groups. Therefore the input spectra, used in the SAND II calculations, are modified in the 14.0–14.1 MeV energy range, where the flux density is assumed to increase by an extra factor 50 [5]. The unfolded spectra are shown in fig. 7 (curve 1, 11 iterations $D = 5.98\%$, curve 2, 8 iterations, $D = 5.37\%$; curve 3, 12 iterations, $D = 6.33\%$).

The ratios of the measured to calculated activity

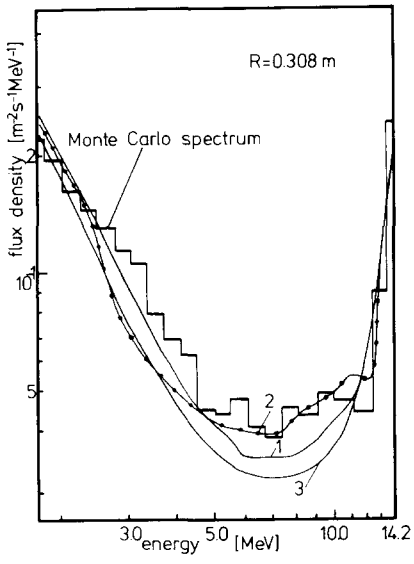

Fig. 6. Results of three SAND II runs and the calculated Monte Carlo spectrum for the position $R = 0.308$ m in the lithium blanket. 1/2 denotes a change of the input spectrum, 1/3 a change of the library.

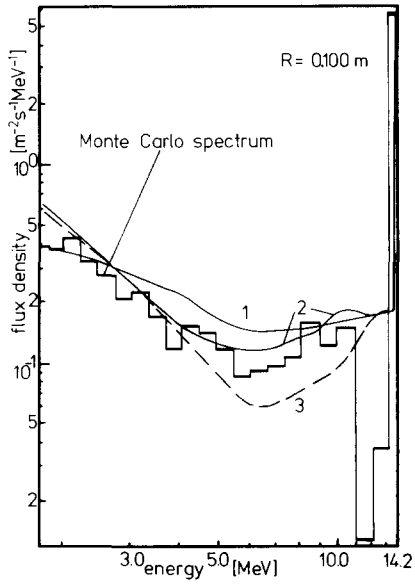

Fig. 7. Results of three SAND II runs and the calculated Monte Carlo spectrum for the position $R = 0.10$ m in the lithium blanket. 1/2 denotes a change of the input spectrum, 1/3 a change of the library.

TABLE 5

Deviations from unity of the rations of measured to calculated activity, obtained by the SAND II program.

Reactions	$R = 0.100$ m input 2 (%)	$R = 0.308$ m input 2 (%)	$R = 0.528$ m input 2 (%)
$^{7}Li(n,\alpha n')t$	−6.30	5.86	6.69
$^{19}F(n,2n)^{18}F$	−1.17	− 3.61	− 7.67
$^{24}Mg(n,p)^{24}Na$	−0.83	− 7.52	−10.21
$^{27}Al(n,\alpha)^{24}Na$	7.02	− 3.20	0.53
$^{27}Al(n,p)^{27}Mg$	3.55	0.24	1.67
$^{56}Fe(n,p)^{56}Mn$	−2.74	−12.98	−12.21
$^{58}Ni(n,2n)^{57}Ni$	−6.58	1.19	1.69
$^{58}Ni(n,p)^{58}Co$	−6.60	− 3.45	− 2.78
$^{58}Co(n,\alpha)^{56}Mn$	5.04	14.66	7.45
$^{63}Cu(n,2n)^{62}Cu$	6.21	5.06	5.40
$^{64}Zn(n,p)^{64}Cu$	−5.95	− 4.54	− 2.45
$^{115}In(n,n')^{115m}In$	1.59	1.83	0.27
$^{127}I(n,2n)^{126}I$	6.67	6.47	11.63
Deviation parameter	5.37	7.09	7.05
Number of iterations	8	14	7

for each reaction, obtained by the SAND II program, are listed in table 5.

The agreement between the Monte Carlo spectrum and the unfolded spectrum is relatively good (deviations of about 20% between the flux density values) when the reference blanket spectrum is used as input spectrum.

The spectra, determined with the use of the CCC 112B library, generally show larger deviations. Only at the position $R = 0.10$ m can large deviations be observed in the 11–14 MeV energy range, which has probably two reasons. At first, the resolution of the unfolding method is not so good that this kind of dips in a spectrum will be calculated if the shape is not already present in the input spectrum. Secondly, there will be differences between the Monte Carlo calculated neutron spectrum and the spectrum from the target jacket in the experiment, which is disturbed by cooling water supplies, target material etc.

In order to get some numerical data on the influence of the uncertainties in the activities and in the cross sections, a Monte Carlo error analysis was performed; this error analysis is based on a description by Oster[17]). The uncertainties in the measured activities are given in table 1; furthermore the evaluated cross section error values from McElroy[18]) were applied. Since these values have not been published for the $^{7}Li(n,\alpha n')t$, the $^{19}F(n,2n)^{18}F$ and the $^{59}Co(n,\alpha)^{56}Mn$ reaction, these three reactions were deleted in the error analysis. However, since the cross section error values are only published for the reactions from the CC 112B library the results of this investigation cannot be related to the calculated best output spectrum, obtained with the "ENDF/B-IV+CCC 112B" library. This should thus be considered as a calculational experiment, showing the influence of uncertainties in activities and cross sections. For the input-spectrum only the reference blanket spectrum is taken.

In one series of calculations only the random errors in the activity values are considered, while in another series both random errors in the activity values and errors in the cross section data are taken into account, following Oster's procedure. The program applied is a modified version of SAND II, the SANDPET [19]) program.

For each of the three positions in the lithium blanket ten SAND II runs were made applying the procedure mentioned above. The results of both approaches are presented in the figs. 8–10. In each of the figures the average value of the SAND II runs is plotted as well as two curves denoting two times the standard deviation in this solution by

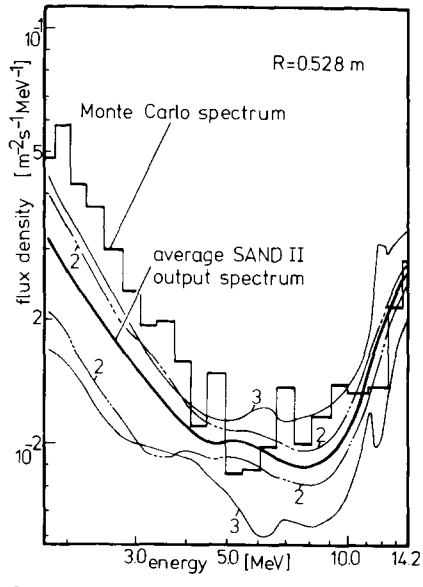

Fig. 8. Comparison of the calculated Monte Carlo spectrum and the average output spectrum obtained from 10 SAND II runs for the position $R = 0.528$ m. On both sides of this spectrum two curves are given at a distance of two standard deviations in the average value, assuming: (a) only errors in the activity values (curves 2); (b) both errors in the activity values and in the cross sections (curves 3).

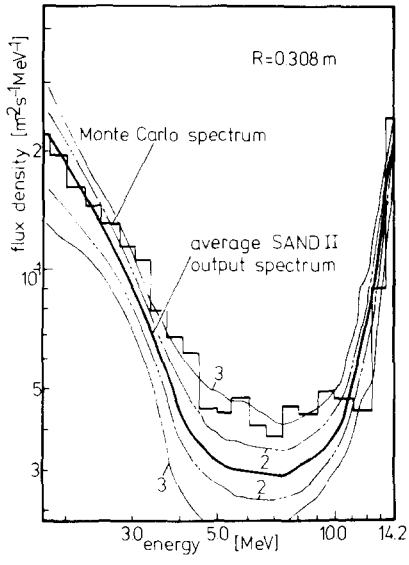

Fig. 9. Equal curves as described under fig. 8 for the position $R = 0.308$ m.

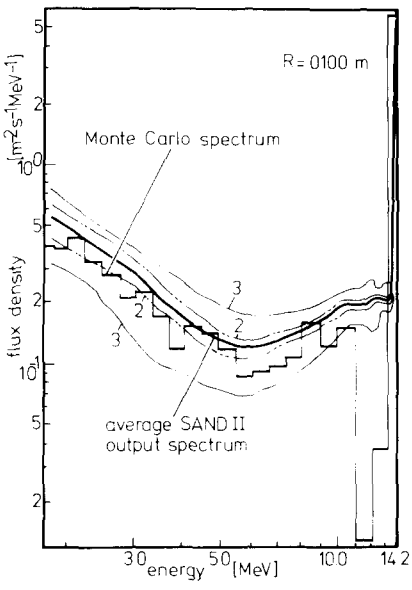

Fig. 10. Equal curves as described under fig. 8 for the position $R = 0.100$ m.

varying either the activities or both the activities and the cross sections.

Although performed as a calculational experiment, it is shown clearly by this analysis that deviations between MORSE calculated and SAND II evaluated neutron spectra may be mainly due to errors in the applied cross sections combined with uncertainties in measured activities.

However, from the results above it can be concluded that the activation technique offers, up till this moment, one of the best chances to determine fast neutron energy spectra in CTR-experiments.

The authors are grateful to Drs. W. L. Zijp and Mr. H. J. Nolthenius, ECN Petten, Netherlands, who kindly supplied them with the unfolding program and the cross section data files. They also wish to thank Dr. N. Kirch for his helpful remarks and Mr. J. Gelissen for operating the neutron generator.

References

[1] I. E. Struve and N. Tsoulfanides, Nucl. Technol. **21** (1974) 201.
[2] D. E. Bartine et al., Nucl. Sci. Eng. **53** (1974) 304.
[3] H. Dederichs, Thesis (RWTH Aachen, Germany) to be published.
[4] P. Cloth et al., Nucl. Instr. and Meth. **124** (1975) 305.
[5] L. J. M. Kuijpers, Thesis published (EUT Eindhoven, Netherlands, November 1976) (also published as Jül-1356).
[6] B. Chinaglia and R. M. Malvano, Nucl. Instr. and Meth. **105** (1966).
[7] W. N. McElroy et al., AFWL-TR-67-41, vol. 1, 2, 4 (1967).
[8] J. M. Keller and W. P. Voorbraak, private communications (RMG Note 73/11, RCN Petten, 1973).
[9] H. Ch. Rieffe and H. J. Nolthenius, private communications (RCN-75-157, RCN Petten, 1975).
[10] T. Shiokawa et al., J. Inorg. Nucl. Chem. **30** (1968) 2.
[11] E. Stranker et al., The MORSE code, ORNL-4585 (1970).
[12] R. Wright et al., SUPERTOG 3, ORNL-TM-2679 (1967).
[13] R. Herzing, Thesis published (RWTH Aachen, Germany), December 1976 (also published as Jül-1357).
[14] R. Dierckx, Nucl. Instr. and Meth. **107** (1973) 397.
[15] R. Herzing et al., Nucl. Sci. Engng. **60** (1976) 169.
[16] C. M. Lederer et al., *Table of isotopes* (6th ed.; J. Wiley, New York, 1967).
[17] C. A. Oster et al., HEDL-TME-73-20 (1974).
[18] W. N. McElroy and L. S. Kellogg, Nucl. Technol. **25** (1975) 330.
[19] W. L. Zijp and H. J. Nolthenius, private communications (Progress Report ECN-76-109, June 30, 1976).